

May 13, 1988

Finite Element Analysis of NC-9 Dipole
Note #1
Model Description

Bob Wands and Mike Chapman

Introduction

This report describes the ANSYS finite element model that has been generated to examine the behaviour of a two-dimensional cross section of an NC-9 dipole magnet under assembly, cooldown, and electromagnetic loads. The model is highly detailed, geometrically accurate, and provides considerable flexibility in the representation of material properties and component interaction. Early results with simplified material behaviour assumptions show very good agreement with experimental measurements.

Analysis Program

The ANSYS general purpose finite element program was chosen for model generation and solution because of its broad range of capabilities, strong acceptance in the finite element community and excellent documentation and support. Very general material properties and interface behaviour can be modeled with relative ease. Powerful post-processing is available to simplify the task of understanding the interactions of dipole components.

General Model Characteristics

The model of the collars and coils is shown in Fig. 1 with some portions of the collar mesh omitted for clarity (see below). It represents a two-dimensional cross section of an NC-9 dipole far from the ends, with an axial depth of 1 inch. Bilinear interface elements ("gaps") which support compressive contact only are used along those surfaces where separation is a possibility. Approximately 1900 nodes and 1500 elements are used, with a maximum wavefront of 167.

Components of the Finite Element Model

Collars

The collars were based on the geometry of Drwg. 22H0524, Rev. A. Four individual and identical collar pieces, stamped from 7075-T6 Al, are required to provide 360 degrees of coverage. The individual collar pieces are connected

by rods inserted through holes in the collars, and by nickel steel keys inserted in the keyways of the interlocking collar portions, as shown in Fig. 2. In addition, there is an interaction of the tang of one collar with the slot of its mating piece when there are loads acting which tend to expand the collar radially outward. In order to correctly represent the interaction of the four-piece collar unit, the model uses two distinct collar meshes. The first, referred to as the front collar, is shown in Fig. 3. The second, referred to as the back collar and tang, is shown in Fig. 4. Each mesh consists of ANSYS STIF42 plane stress quadrilaterals with a thickness of 0.5 in. Constraint equations are applied along the vertical and horizontal planes as indicated in the figures. The modeling of the back collar and tang allows these pieces to interact in compression along the line shown.

There is, by design, a mismatch in the angles of the key and keyway tapers which tends to evenly distribute the keying force on the keyway. The model includes key elements, which interact with the appropriate surfaces of the front and back collar meshes through "gap" elements. The taper mismatch is modeled by specifying initial gap openings corresponding to the clearance provided by the mismatch.

The interaction of the front and back collars through the hole is accomplished with gap elements, oriented radially between the pin and the holes on the collars. This allows frictionless rotation and radial movement consistent with hole and pin tolerance.

Coils

The coil geometry was based on the mesh used in the Lorentz force calculations of S. Caspi and M. Helm, and documented in SSC-MAG-159. Each conductor was represented by three ANSYS STIF42 quadrilateral elements of unit depth, as shown in Fig. 5. This allows the Lorentz forces to be input to the stress analysis with the same resolution with which they were calculated. Each individual conductor is defined with nodes unique to itself, and with nodal degrees of freedom tangent to the interface between conductors. Therefore, each conductor can be modeled as capable of sliding without friction relative to its neighbors, or fully coupled to act as a homogenous unit. Orthotropic properties can be specified in the radial and azimuthal directions of the conductors.

Interfacing Solid

The actual dipole coils are surrounded by various layers of material in the space between the inner and outer coil, and the coils and collars. This is shown in Fig. 6. Depending upon the location, this material may be kapton, brass, G-10, stainless steel, teflon, or copper. For the purposes of this analysis, this space is filled with ANSYS STIF42 quadrilaterals and triangles to form an

interfacing solid. This solid is broken up into four independent pieces, as shown in Fig. 7, which is an approximation to the actual application of the interfacing material layers.

The material properties of this solid are felt to be of little importance. This is because in the radial direction it's thin dimension will make it considerably stiffer than the surrounding coils and collar with which it is in series, and in the azimuthal direction, it's long, thin shape will contribute little to the stiffness of the coil and collars with which it is in parallel. In both cases, the solid will have little effect on structural stiffness.

Interface Characterization

There is the possibility of significant sliding between the inner and outer coil and between the coils and the collars along the boundary between these components as defined by the interfacing solid. The modeling of this behaviour is provided for by using coincident and independent nodes on these boundaries, as was done with the individual conductors described above. It is then possible to use gap elements and complete or partial nodal coupling to allow the surfaces to separate, slide without friction, or act as though they are "glued" together.

The interfaces along which these types of behaviour can be modeled are shown in Fig. 8.

Material Properties

The material properties of the aluminum collars are well known, and those of the interfacing solid are thought to be of negligible importance. The least understood material behaviour is that of the coils themselves. Compressive load-deflection testing shows an effective Young's modulus which varies from $0.5(10^6)$ psi at stresses of a few thousand psi to $1.5(10^6)$ psi at stresses of about ten thousand psi. The collaring loads occur across this stress range, and simple, constant property assumptions are clearly approximate.

In addition to the non-linear modulus, there is evidence of permanent deformation (plasticity) as well as time-dependent deformation (creep and material damping). Inclusion of these non-conservative effects requires that the load history of the assembly procedure be well defined, since the solution is no longer a function of the final state alone, but also the path taken to reach it.

The modeling of the conductor material properties is limited by both the quantification of those properties and the ability of the ANSYS program to represent them. Fully non-linear, non-conservative analyses represent a large

expenditure of time and effort, and can only be justified if a linear elastic model is suspected of producing significant error. The definition of "significant error" is itself a matter of debate, and given the difficulty of measuring forces and deflections within the coils of real dipoles, verifying that any model is reasonable is no small task.

Loading

The dipole is subjected to three distinct types of loading.

1. Assembly Loads

The first of these loads occurs when the collars are placed around the pre-wound coils and brought together so that the retaining keys can be inserted. Because the coils are manufactured with an azimuthal dimension (arc length) which is slightly greater than that provided by the portion of the collar in which they rest, this procedure produces compressive hoop (azimuthal) stresses in the coils (and tensile stresses in the collars) which aid in preventing collar/coil separation under subsequent Lorentz force loading. These hoop stresses have been measured in prototype magnets using strain gauge devices which give an average value in the coils. However, early finite element results show that there may exist considerable gradients of this stress from the inner to the outer radius of a coil. Therefore, current thinking favors applying the collaring loads to the finite element model with specified displacements at the midplane of the magnet. This is consistent with the displacement controlled nature of the collaring process, and does not produce the artificial uniformity that an applied midplane hoop pressure would yield.

Following the collaring, the collar/coil assembly is compressed on its horizontal midplane sufficiently to allow insertion into the iron yoke. This yoke (not included in the model presented in this report) contacts the collar/coil assembly through a shim on the horizontal midplane, and provides additional stiffness against Lorentz forces. This is also a displacement-controlled loading, and will be modeled with specified interferences between the yoke and collar.

2. Cooldown Loads

The cooldown to superconducting temperature (approx. 4.3K) produces thermal stresses due to thermal gradient during the cooldown, and differences in the thermal contraction coefficients of the collars and the coils. Temperature-dependent thermal conductivity, thermal contraction, and Young's modulus definitions, as well as time-dependent load stepping should allow reasonable approximation to the cooldown scenario.

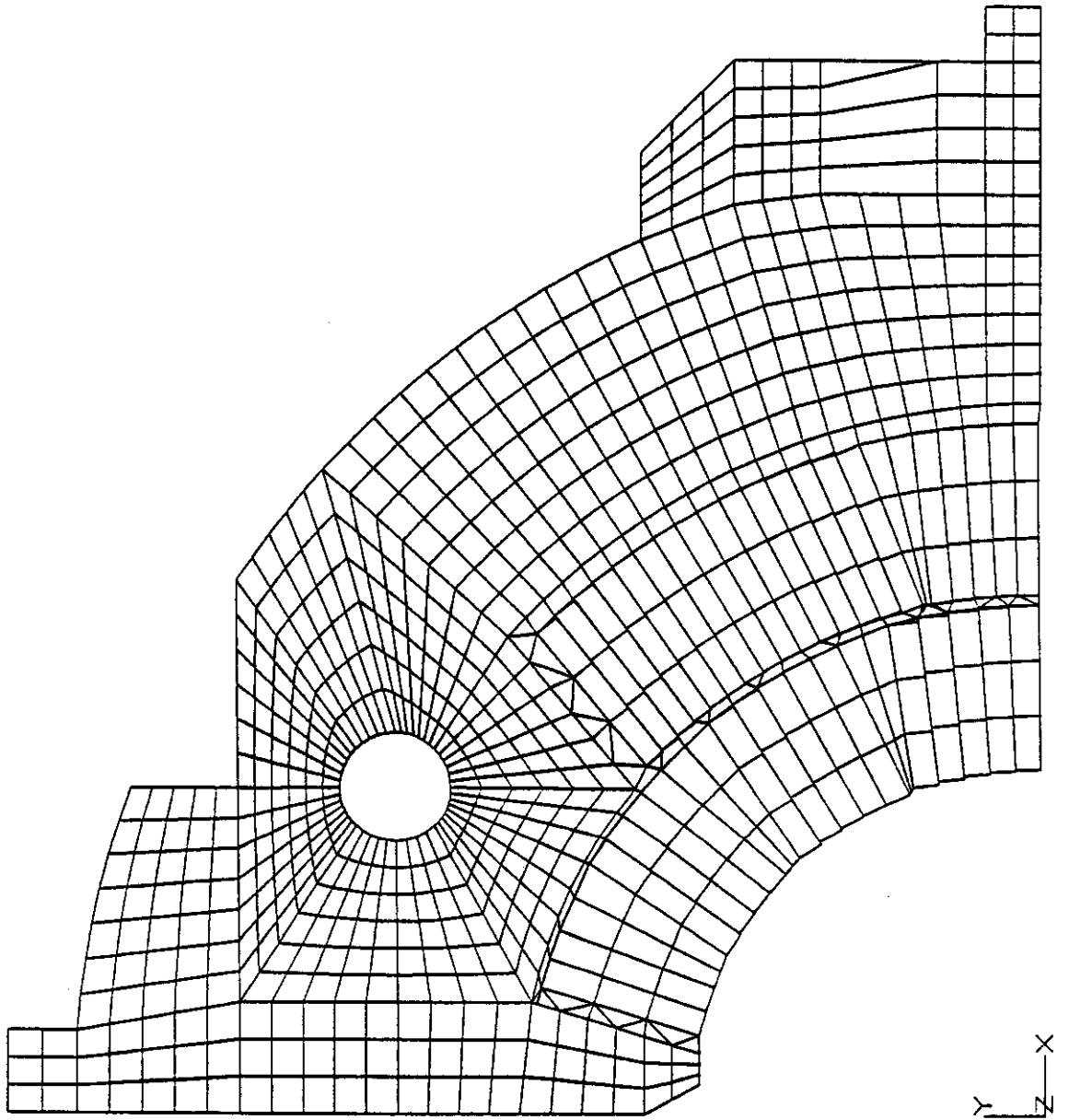
3. Lorentz Forces

The charging of the magnet to its operating current produces Lorentz forces due to the interaction of the current flux and the magnetic field. Two dimensional magnetostatic analysis has provided three values of Lorentz force for each conductor, documented in the report by Caspi and Helm referenced above. These forces will be input as concentrated forces on the conductor nodes.

ANSYS 4.3
MAY 17 1988
14:33:51
PLOT NO. 1
PREP7 ELEMENTS

ORIG
ZV=1
DIST=1.39
XF=1.26
YF=1.16

Fig 1. Finite Element Mesh
of SSC NC-9
Dipole Cross Section



1 THE MOTHER OF DP MODELS

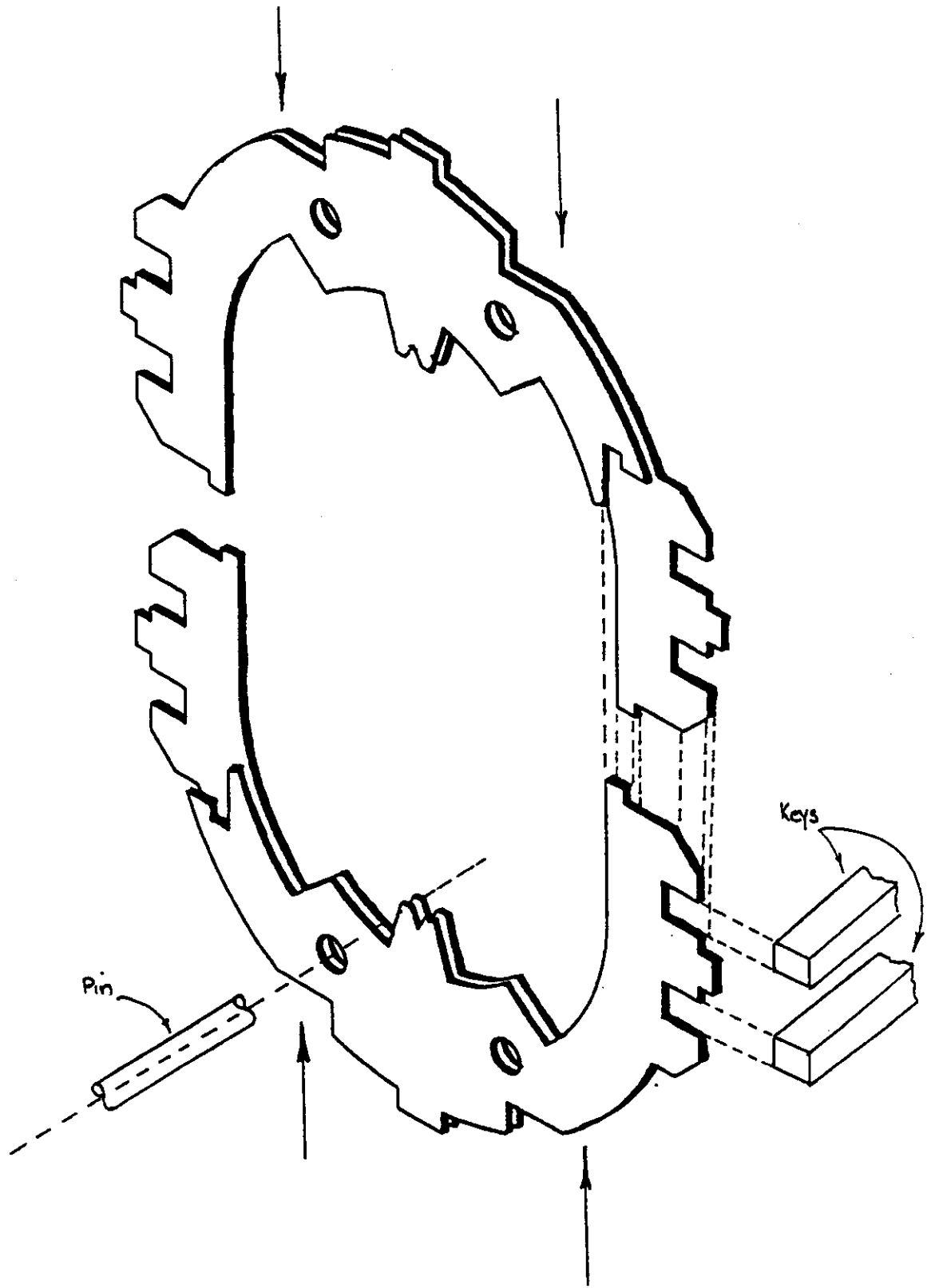
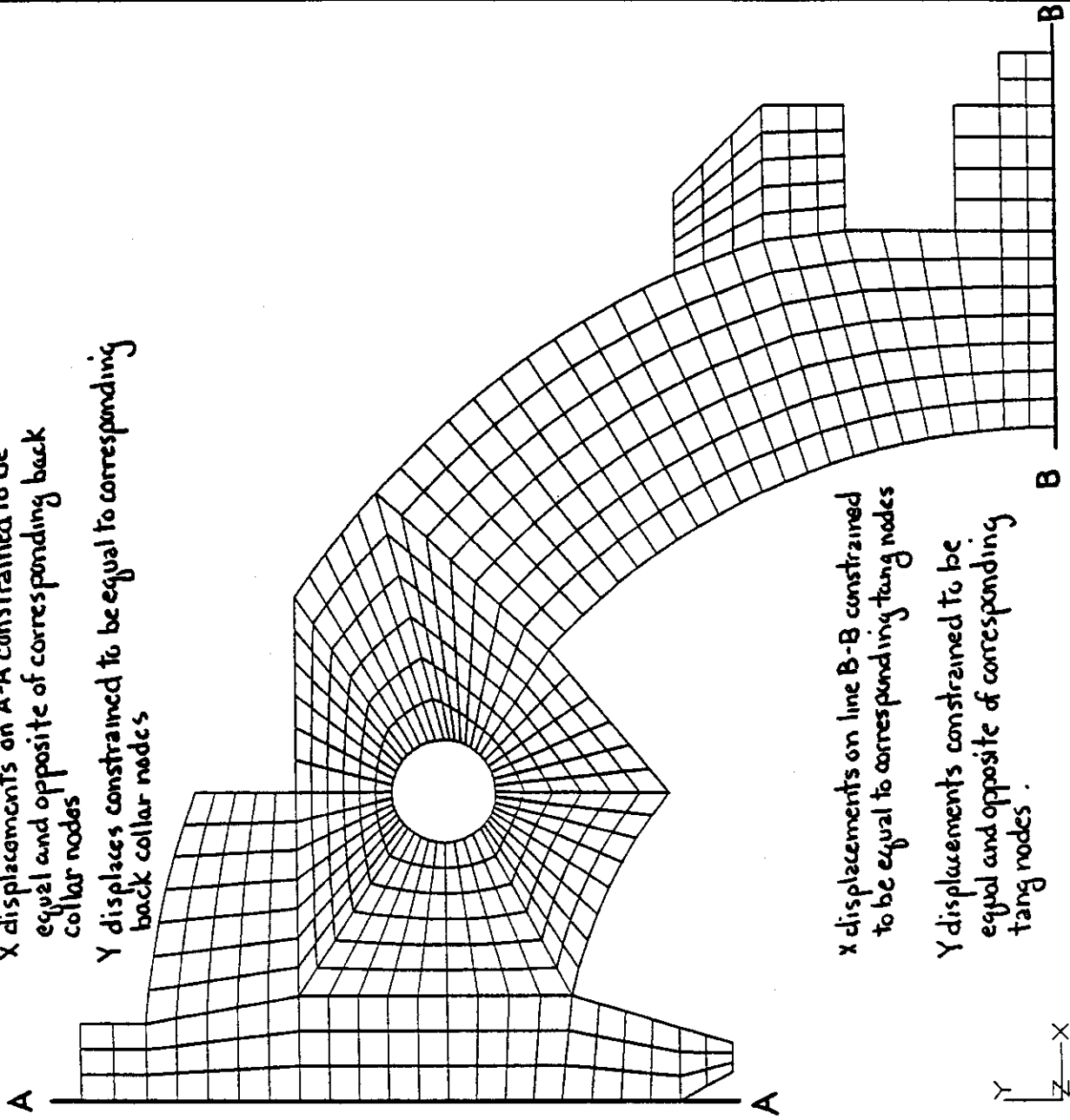


Fig2. Interlocking of four collar pieces

X displacements on A-A constrained to be equal and opposite of corresponding back collar nodes
 Y displacements constrained to be equal to corresponding back collar nodes



X displacements on line B-B constrained to be equal to corresponding tang nodes
 Y displacements constrained to be equal and opposite of corresponding tang nodes.

ANSYS 4.3
 MAY 18 1988
 7:12:24
 PLOT NO. 1
 PREP7 ELEMENTS

ORIG
 ZV=1
 DIST=1.39
 XF=1.26
 YF=1.16

Fig3. Mesh of Front Collar

ANSYS 4.3
MAY 17 1988
14:34:25
PLOT NO. 3
PREP7 ELEMENTS

ORIG
ZV=1
DIST=1.39
XF=1.26
YF=1.16

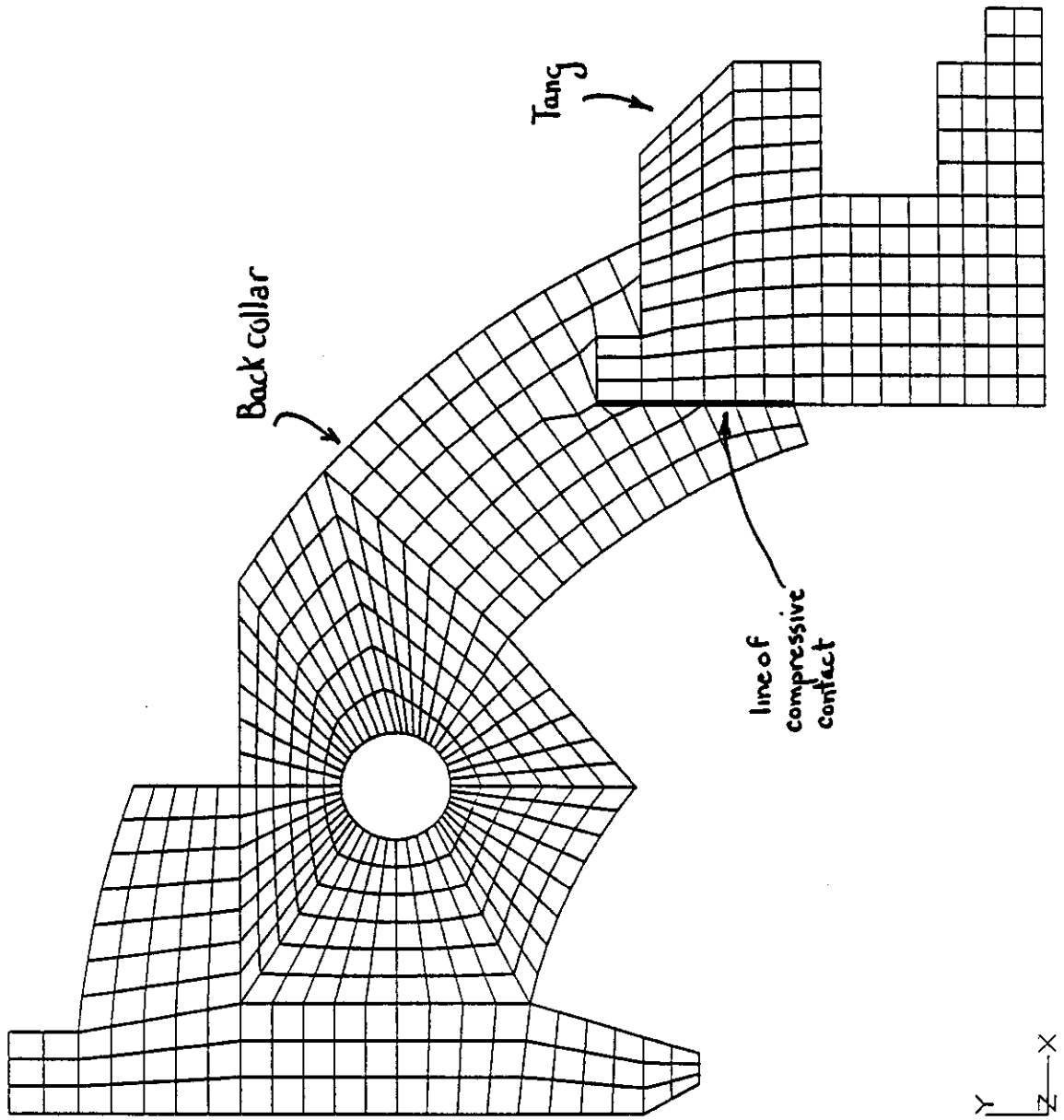


Fig 4. Mesh of Back Collar and Tang

ANSYS 4.3
MAY 17 1988
14:34:21
PLOT NO. 2
PREP7 ELEMENTS

ORIG
ZV=1
DIST=.769
XF=.88
YF=.571

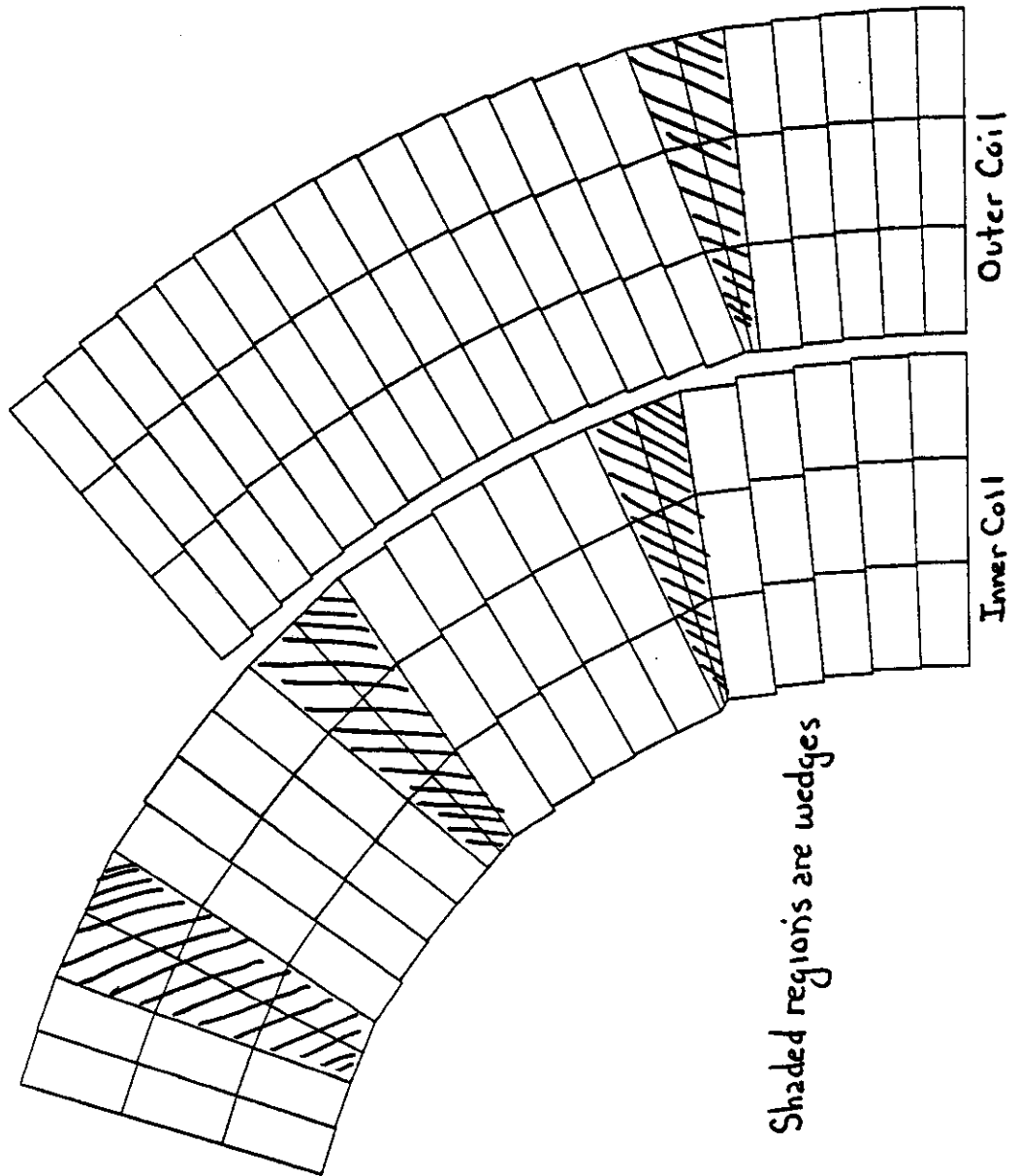


Fig 5. Coil Mesh

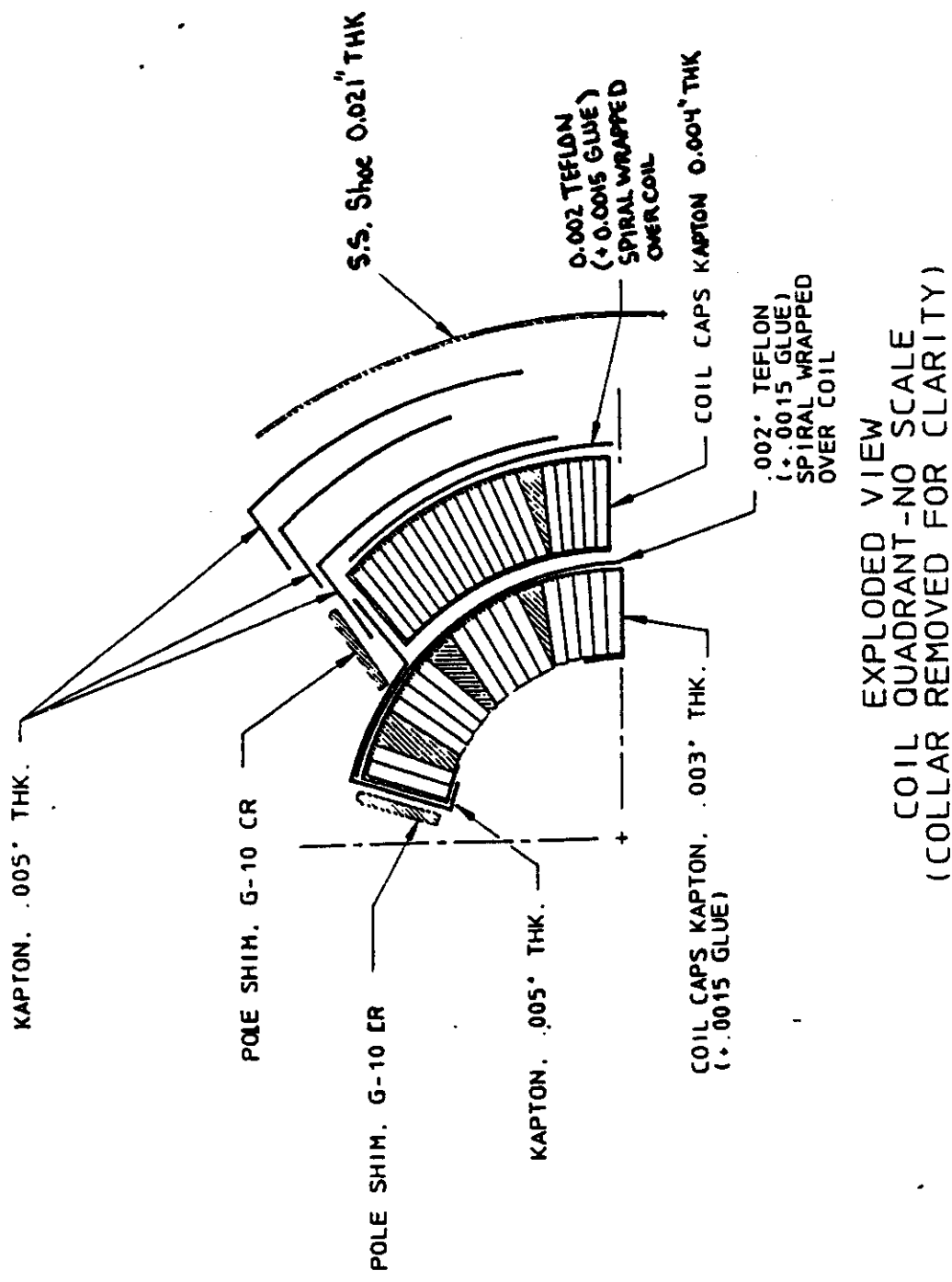
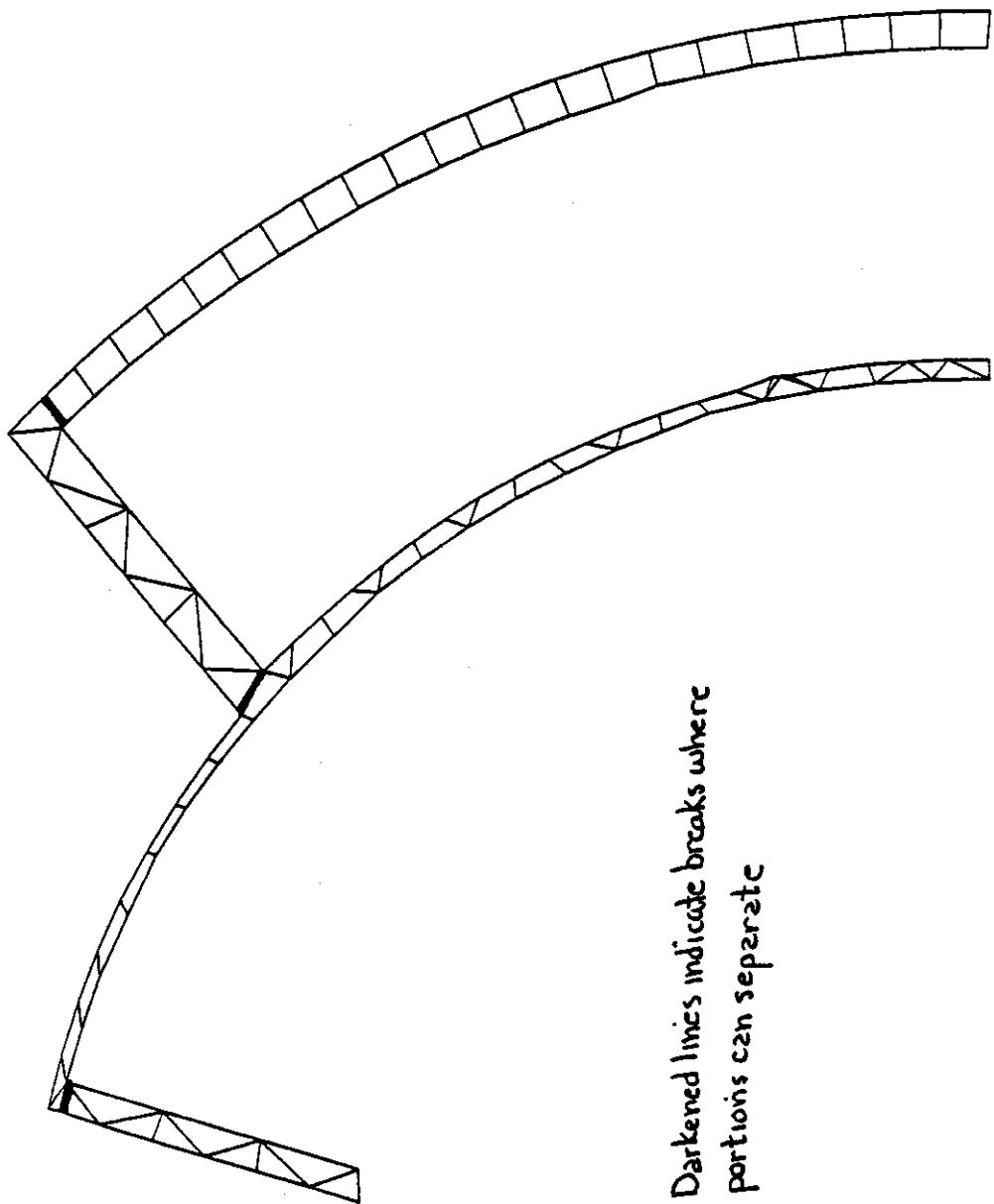


Fig 6. Coil Detail Showing Material Layers around Coils

ANSYS 4.3
MAY 18 1988
10:27:03
PLOT NO. 1
POST1 ELEMENTS

ORIG
ZV=1
DIST=.817
XF=.883
YF=.602



*Darkened lines indicate breaks where
portions can separate*

*Fig 7. Interfacing Solid
Mesh*

ANSYS 4.3
 MAY 17 1988
 14:33:51
 PLOT NO. 1
 PREP7 ELEMENTS

ORIG
 ZV=1
 DIST=1.39
 XF=1.26
 YF=1.16

Darkened lines indicate interfaces along which elements may slide, separate, or act as fully coupled, depending upon input

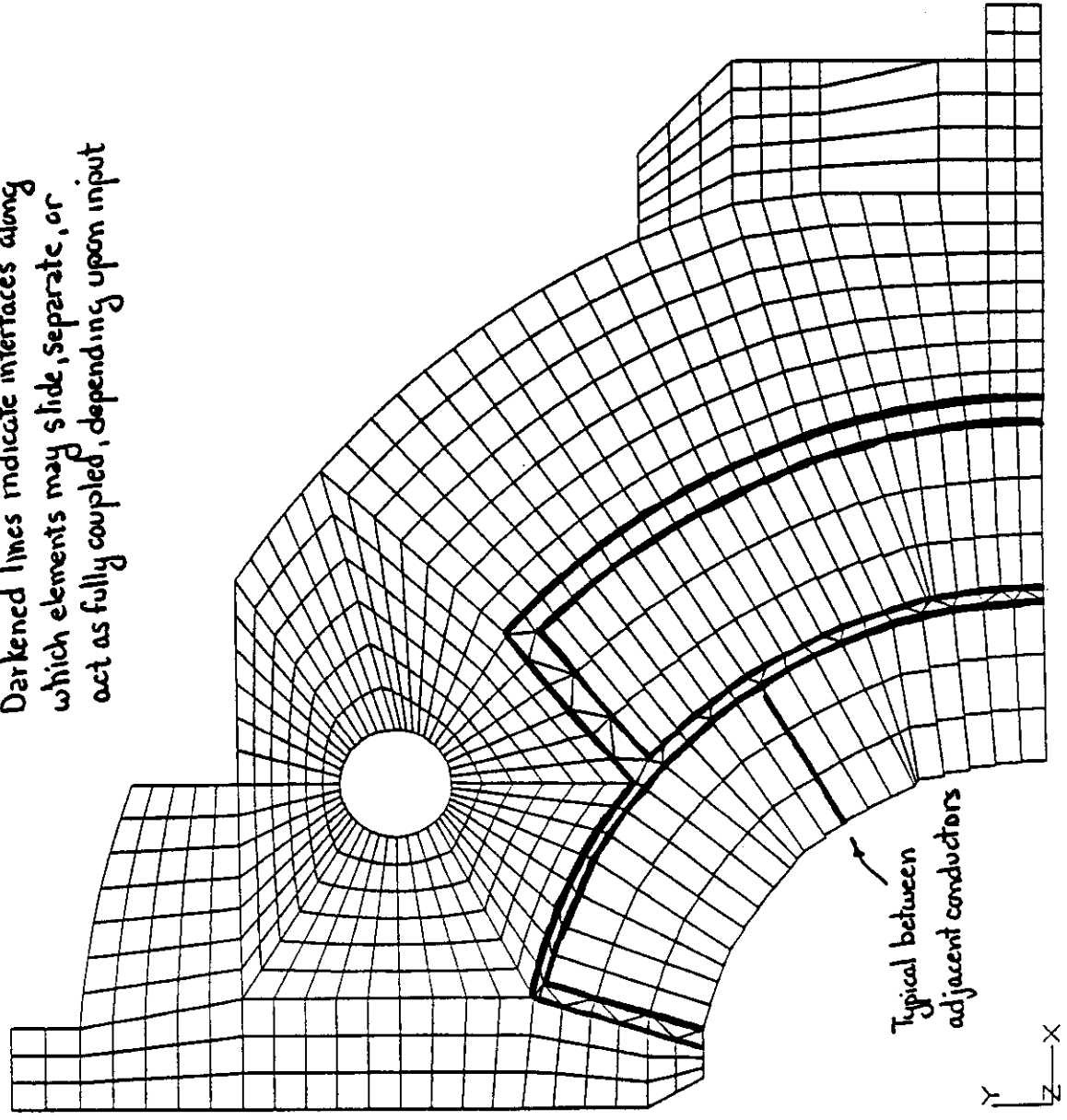


Fig 8. Interface Characterization